THE GEOCHEMISTRY OF BANDED IRON FORMATIONS IN THE SUKUMALAND GREENSTONE BELT OF GEITA, NORTHERN TANZANIA: EVIDENCE FOR MIXING OF HYDROTHERMAL AND CLASTIC SOURCES OF THE CHEMICAL ELEMENTS

MAH Maboko
Department of Geology, University of Dar es Salaam
P.O. Box 35052, Dar es Salaam, Tanzania

ABSTRACT

Major and trace element compositions of samples of Banded Iron Formations (BIF) from the Neoarchaean Sukumaland Greenstone Belt of Geita in northern Tanzania reveal that the BIF precipitated from hydrothermal solutions. Fe-Ti-Al-Mn systematics suggest that the hydrothermal deposits have been contaminated, by up to 20% by weight, with detrital material having a composition similar to modern deep-sea pelagic clays. SiO_2 and Fe_2O_3 contents are 48.2 to 88.5% and 8.9 to 49.1% respectively. Al_2O_3 contents lie between 0.33 and 2.1% and show no correlation with either Fe_2O_3 or SiO_2. Al_2O_3 is, however, positively correlated with Ti, Ga, Hf, Rb, Th, Zr and Sr but not with CaO, the alkalies and the total Rare Earth Elements (REE). The other major element oxides are generally present in negligible amounts. The samples are characterised by mean Zr/Hf and $^{144}Sm/^{143}Nd$ ratios of 48± 5 (2 SE) and 0.10±0.01 (2 SE) respectively, similar to mean upper continental crustal values. Shale-normalised REE patterns are nearly flat, except for small positive Eu and very slight negative Ce anomalies and reveal that, compared to average upper crust, the abundances of the REE in the BIF are up to an order of magnitude lower. Chondrite-normalised patterns are characterised by light (L) REE enrichment, flat to slightly depleted heavy (H) REE, slightly positive Eu anomalies and very small negative Ce anomalies. The HREE-depleted patterns are similar to patterns derived from granite-dominated upper continental crust and indicate that the bulk of the REE in the Geita BIF can not have been derived from a mixture of Neoarchaean sea water and bottom hydrothermal solutions. The trace element data, and the REE in particular, indicate that, despite their relatively low proportions, granitic

*detritus probably derived from contemporaneous felsic flows
and pyroclastics are the cause of the dominant trace element
geochemical signature of the BIF.*

INTRODUCTION
Banded Iron Formations (BIF) are marine chemical precipitates that form an integral part of the preserved Archaean to Proterozoic sedimentary succession in different parts of the world. In general, two main types of BIF can be distinguished. The Superior-type BIF, which are dominant in the Proterozoic, are characterised by shallow continental shelf sedimentary associations whereas Algoma-type BIF occur in close association with mafic and felsic volcanic rocks, graywackes and carbonaceous shales in small sedimentary basins in many Mesoarchaean greenstone belts (Klemm 2000).

The origin of the Fe and Si that constitute the bulk of the BIF remains contentious. Some researchers contend that the Fe and Si are of terrigenous origin, having been derived from land by weathering processes (James 1954, Lepp & Goldich 1973, Garrels 1987, Holland 1984, Halbich *et al.* 1993). Two variants of the terrigenous origin are generally advocated. The first variant assumes that these elements are carried directly into the oceans as dissolved matter in river water (James 1954). The second variant assumes that the elements are leached from the suspended load of rivers after deposition in the deeper, more reducing part of the ocean (Holland 1984). Other workers, however, favour a volcanogenic hydrothermal origin for most of the elements in BIF (Goodwin 1962, Jacobsen & Pimentel-Klose 1988, Barley *et al.* 1997). The hydrothermal origin, an analogue of which are the hydrothermal systems operating along modern mid-ocean ridges, is particularly favoured for the Algoma - type BIF because of their strong association with volcanic and/or volcanoclastics rocks (Jacobsen & Pimentel-Klose 1988).

Regardless of the ultimate source of the constituent chemical elements, detritus-poor BIF are useful indicators of the temporal evolution of sea water chemistry and the physico-chemical conditions that have influenced its composition from Archaean to Proterozoic times. In particular, REE geochemistry has been used to put some constraints on the various geochemical fluxes that have influenced seawater chemistry in the past (Jacobsen & Pimentel-Klose 1988, Derry & Jacobsen 1990, Bau & Moller 1993). This in turn has allowed researchers to infer the physical-chemical processes that had controlled marine chemistry during Precambrian time (Derry & Jacobsen 1990, Bau & Moller 1993).

The Neoarchaean Sukumaland Greenstone Belt (Borg 1992, Borg & Shackleton 1997) of northern Tanzania contains a well developed sequence of typical Algoma-type BIF that occur in close association with metabasalts, carbonaceous shales, felsic flows and pyroclastics. This paper presents the

first ever-published geochemical data on samples of BIF from the Sukumaland Greenstone Belt in the northern part of the Tanzania craton (Fig. 1). Because of problems with getting easily accessible fresh exposures sampling was restricted to a relatively small area surrounding the old Geita Mine were unaltered samples could be obtained from mine addits, quarries, artisanal miners' pits and road cuts. The data are used to place some constraints on the sources contributing to the major and trace element geochemical budget of the late Archaean sea from which the BIF were deposited. The term iron formation as used in this paper includes samples with Fe concentrations below the 15% lower limit proposed by James (1954).

GEOLOGICAL SETTING

The Sukumaland Greenstone Belt consists of two intermittently exposed arcs of metavolcanic and metasedimentary rocks which are cored and flanked by granitoids and gneisses in the area south of Lake Victoria (Fig. 1). In terms of the local stratigraphy, rocks of the Sukumaland Greenstone Belt belong to the Nyanzian Supergroup (Grantham *et al.* 1945). The Nyanzian has been subdivided into a Lower part consisting predominantly of mafic metavolcanics and an Upper part consisting of chemical metasediments, including chert and BIF, felsic tuffs and flows, agglomerates and graphitic shales (Barth 1990). The Upper Nyanzian is uncomformably overlain by coarse clastic metasediments of the Kavirondian Group (Barth 1990).
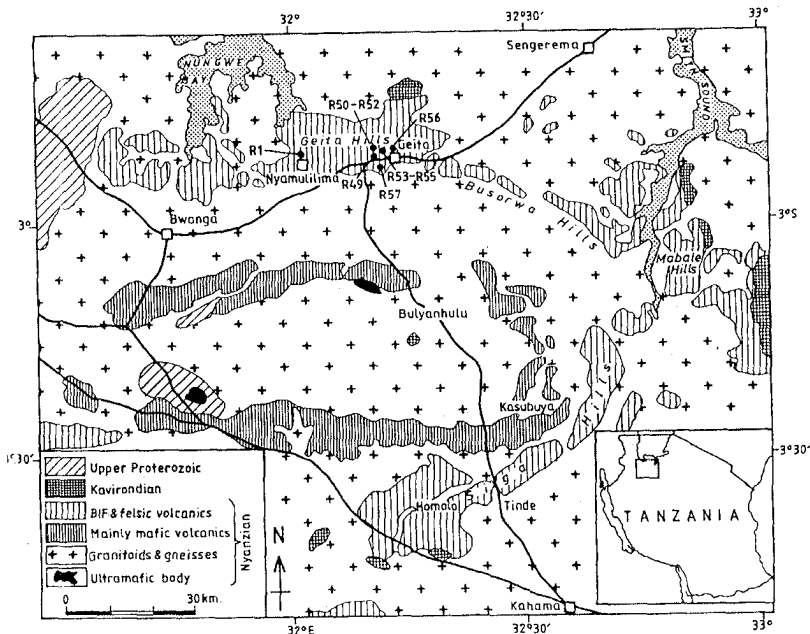

Fig. 1: Geological sketch map of the Sukumaland Greenstone Belt showing sampling localities (modified from Borg and Krogh 1999). Sampling localities are indicated by dots and numbers.

The geological setting and lithostratigraphical subdivisions of the Sukumaland Greenstone Belt has been reviewed by Barth (1990), Borg (1992) and Borg and Shackleton (1997). These workers demonstrated that the inner arc of the Sukumaland Greenstone Belt is representative of the Lower Nyanzian whereas the outer arc, from where the samples studied herein were obtained, represents the Upper Nyanzian (Fig. 1). Walraven *et al.* (1994) described the BIF at Geita as belonging to the oxide facies and recognised three distinct lithofacies: a basal magnetite-haematite-chert lithofacies consisting of micro- and meso-banded magnetite-haematite and chert with Fe-Si oxide ratios ranging from ~4:1 at the base to ~1:3 at the top. This lithofacies grades into an overlying banded chert lithofacies with rare mafic to intermediate tuffaceous interlayers separating the two units locally. The chert lithofacies consists of banded chert interbedded with up to 50 cm thick layers of white and red felsic tuffs. Only minor magnetite-rich layers or laminae occur in the chert beds. The upper most lithofacies is a transitional unit in which chemical and pyroclastic metasediments alternate. The tuff layers become more abundant and thicker towards the top of the unit.

Drilling at Nyamulilima Hill (Fig. 1) has established a local stratigraphy consisting of an upper unit of felsic tuff underlain by BIF (Manya pers. comm.). The BIF, which attains a maximum thickness of ~70 m, overlies graphitic shales consisting of coarse nodules of pyrite. The BIF forms prominent crests and ridges overlying the more easily weathered shales and pyroclastics and consists of rhythmically alternating fine bands of Fe-oxide and metachert metamorphosed into the greenschist facies. The metachert layers consist of a fine-grained granoblastic mosaic of quartz interspersed with varying proportions of Fe oxide whereas the oxide layers consists of a mixture of magnetite and haematite with no silicate minerals. The presence of oxide even in the nominally chert layers and the absence of quartz in the haematite-magnetite layers suggest that the rhythmic banding represents repeated cycles of Si deposition superimposed on a more or less constant flux of Fe oxide deposition. Carbonates and sulphides are generally absent except in a few samples where they occur as secondary minerals mostly in cross cutting veins. Massive sulphide-rich layers, up to 4 m thick and thin sulphide rich tuffaceous horizons are, however, locally interbedded with the BIF. Observations in drill cores reveal the presence in the massive sulphide layers of BIF fragments, lapilli and detrital pyrite cores, often overgrown with secondary pyrite, suggesting a pyroclastic origin for the layers. The BIF beds show tight isoclinal folding, very steep ($\geq 70°$) dips and along strike orientations, which are controlled by the local geometrical pattern of the folding.

The deposition age of the BIF is constrained by a zircon U-Pb age of 2699 ± 9 Ma reported by Borg and Krogh (1999) from a porphyritic trachyandesite flow intercalated with BIF at the Geita mine.

Analytical Methods

Ten BIF samples collected from the area around Geita (see Fig. 1 for sampling localities), were analysed for major and trace elements at the ACME Analytical Laboratories in Vancouver, Canada. Aliquots of the pulverised samples, mixed with $LiBO_3$ flux, were melted prior to acid digestion. The major elements, were analysed using Inductively Coupled Plasma-Optical Emmission Spectrometry (ICP-OES) whereas the trace elements were determined using Inductively Coupled Plasma-Mass Spectrometry (ICP-MS). The analytical reproducibility as determined from duplicate analyses is better than 4% and typically ~2.5% for trace elements and better than 0.2% for major elements. The accuracy of the ICP-MS measurements as calibrated against standard samples was better than 2%.

RESULTS

The analytical data for the BIF samples are presented in Table 1. As expected from the petrography, the BIF are almost pure SiO_2 - Fe_2O_3 (all Fe expressed as Fe^{3+}) mixtures with (SiO_2 + Fe_2O_3) ranging from 92.9 to 98.9%. SiO_2 and Fe_2O_3 contents are 48.2 to 88.5% and 8.9 to 49.1% respectively. Al_2O_3 contents lie between 0.33 and 2.1% and show no correlation with either Fe_2O_3 or SiO_2. Al_2O_3 is, however, positively correlated with Ti, Ga, Hf, Rb,Th, Zr and Sr but not with CaO, the alkalies and the total REE. The lack of correlation of Al_2O_3 with CaO and the alkalies suggests little input of detrital feldspar in the BIF. The other major element oxides are generally present in negligible amounts except in sample R-51 which contains 0.9% and 1.9% of MgO and CaO respectively (Table 1). In the latter sample, the CaO and MgO most likely reside in carbonate, which is present as a minor phase in the mode.

Table 1: Major (in oxide weight %) and trace element (in ppm) composition of the Geita Banded Iron Formations

Oxide/ Element	R1	R49	R50	R51	R52	R53	R54	R55	R56	R56*	R57	MEAN
SiO_2	88.52	63.55	65.11	62.23	81.52	67.07	48.79	59.41	80.88	80.76	48.23	67.82
Al_2O_3	1.19	1.42	2.1	1.79	0.9	1.24	0.89	1.1	0.34	0.33	0.82	1.10
Fe_2O_3tot	8.91	32.85	30.82	30.71	16.87	30.35	49.08	36.5	17.94	18.11	48.75	29.17
MnO	0.01	0.02	0.01	0.05	0.01	0.01	0.01	0.01	0.01	0.01	0.01	0.01
MgO	0.13	0.04	<0.01	0.92	<0.01	<0.01	<0.01	<0.01	<0.01	<0.01	<0.01	0.36
CaO	0.07	0.09	0.03	1.9	0.07	0.03	0.03	0.02	0.05	0.05	0.09	0.22
Na_2O	0.02	<0.01	<0.01	0.37	<0.01	<0.01	<0.01	<0.01	<0.01	<0.01	<0.01	0.20
K_2O	0.21	0.39	<0.04	0.96	<0.04	<0.04	<0.04	<0.04	<0.04	<0.04	0.13	0.42
TiO_2	0.02	0.05	0.08	0.06	0.02	0.03	0.03	0.04	0.01	0.01	0.02	0.03
P_2O_5	0.05	0.11	0.18	0.15	0.02	0.06	0.1	0.2	0.04	0.11	0.18	0.11
LOI	0.7	1.5	1.5	0.8	0.5	1	0.8	2.5	0.6	0.4	1.5	1.07
Total	99.92	100.07	99.89	100.01	100	99.89	99.82	99.86	99.97	99.89	99.79	99.92
Ba	56	115	39	89	9	13	22	62	40	40	74	50.82
Ni	14.6	6.6	6.5	14.2	16.9	10.4	11.1	10	13.1	12.3	5	10.97

* Duplicate analysis

Table 1 (Continued)

Oxide/ Element	R1	R49	R50	R51	R52	R53	R54	R55	R56	R56*	R57	MEAN
Cu	8.55	14.4	21.4	21.1	7.59	36.4	36.7	36.5	7.5	7.49	3.98	18.33
Ga	2.1	2.8	3.5	3.5	2	2.2	2.4	4	1.7	1.8	1.2	2.47
Hf	0.2	0.3	0.4	0.3	0.1	0.2	0.2	0.3	0.1	0.1	0.1	0.21
Nb	0.55	0.37	0.67	0.58	0.51	0.42	0.48	0.61	0.31	0.34	0.26	0.46
Rb	18.58	21.19	1.67	30.86	0.97	0.97	1.32	1.02	0.61	0.53	13.98	8.34
Sr	74.3	29.5	6.3	106	4.1	4	4.8	88.1	13.7	14	20.7	33.23
Th	0.6	0.5	0.8	0.6	0.5	0.3	0.2	0.6	0.6	0.6	0.2	0.50
U	2.2	0.2	0.6	0.3	7	0.5	0.6	1.5	0.6	0.6	0.1	1.29
Zr	8.2	12.4	18.2	15.2	6.4	8.1	8.9	11.7	5.9	6.2	5.5	9.70
Y	2.5	2.2	3.8	4.8	1.3	2.7	2.4	7.8	2	2.1	2.8	3.13
La	19	6.3	6.2	3.5	2.8	4.1	6.6	21.9	16	15.9	2.4	9.52
Ce	11	6.9	9.6	6.4	3.8	5.5	8.8	38.8	23.8	24.3	2.8	12.88
Pr	2.28	0.76	1.35	0.71	0.54	0.77	0.99	7.37	2.89	2.91	0.52	1.92
Nd	6.7	2.7	5.5	3.4	2	2.9	3.3	37.3	10.2	9.3	2.1	7.76
Sm	0.9	0.4	1	0.6	0.4	0.6	0.5	7.4	1	1.1	0.4	1.30
Eu	0.3	0.18	0.32	0.37	0.12	0.28	0.24	1.67	0.36	0.36	0.2	0.40
Gd	0.85	0.39	0.85	0.73	0.3	0.59	0.56	3.98	0.97	0.94	0.38	0.96
Tb	0.1	<0.05	0.11	0.11	<0.05	0.07	0.07	0.38	0.08	0.08	<0.05	0.13
Dy	0.49	0.27	0.72	0.58	0.24	0.56	0.47	1.72	0.46	0.38	0.38	0.57
Ho	0.09	0.06	0.13	0.13	<.05	0.1	0.08	0.29	0.07	0.06	0.08	0.11
Er	0.25	0.2	0.37	0.42	0.14	0.29	0.23	0.83	0.2	0.19	0.25	0.31
Tm	<0.05	<0.05	0.06	<0.05	<0.05	<0.05	<0.05	0.1	<0.05	<0.05	<0.05	0.08
Yb	0.22	0.2	0.38	0.37	0.13	0.31	0.24	0.57	0.17	0.18	0.23	0.27
Lu	0.04	0.04	0.06	0.04	0.02	0.05	0.04	0.09	0.03	0.03	0.04	0.04
As	1.2	3.6	7	3.9	7.5	4.5	5.8	2.3	2.4	2.4	4.4	4.09
Sb	0.4	2.13	1.94	2.07	1.13	2.37	1.75	1.51	0.43	0.43	0.35	1.32
V	5	14	16	11	14	10	8	39	7	7	2	12.09
Zn	6.2	23.9	6.3	35.6	2.4	3.8	4.2	38.1	4	3.7	5.2	12.13
Co	1.3	1.9	1.9	3.9	2.2	2.5	1.5	2.9	2.5	2.3	1	2.17
Total REE	42.22	18.4	26.65	17.36	10.49	16.12	22.12	122.4	56.23	55.73	9.78	36.14
Fe/Ti	187.2	276.0	161.8	215.0	354.4	425.0	687.3	383.3	753.7	760.8	1024.0	475.3
Al/Al+Fe +Mn	0.092	0.032	0.049	0.042	0.038	0.030	0.014	0.022	0.014	0.014	0.013	0.033
Zr/Hf	41.0	41.3	45.5	50.7	64.0	40.5	44.5	39.0	59.0	62.0	55.0	49.3
Co+Cu+ Ni	24.5	22.9	29.8	39.2	26.69	49.3	49.3	49.4	23.1	22.1	9.98	31.50
Y/P_2O_5	50.0	20.0	21.1	32.0	65.0	45.0	24.0	39.0	50.0	19.1	15.6	34.6

* Duplicate analysis

When compared to post-Archaean average upper continental crust (Taylor and McLennan 1981), the BIF are strongly depleted in the transition metals (Sc and V), REE, High Field Strength Elements (Nb, U, Th, Zr, Hf, Pb),

Large Ion Lithophile Elements (Ba, Sr, Rb) and Y. The mean trace element composition of the BIF (Table 1) is plotted in a Primitive Mantle normalised (Normalising values after McDonough and Sun 1995) spidergram in Figure 2. Apart from overall lower abundances and more pronounced negative anomalies for Nb, Sr, Hf and Ti, the average BIF shows a pattern that is very similar to that of the average upper crust. The only notable differences between average upper crust and the BIF is the strong enrichment of U relative to Th and K in the latter. The BIF pattern is also characterised by positive Nd - P and negative Hf and Zr anomalies which features are absent in the upper continental crust (Fig. 2). Nd is, however, not correlated with P_2O_5 indicating little influence of sedimentary apatite in the REE budget of the BIF.
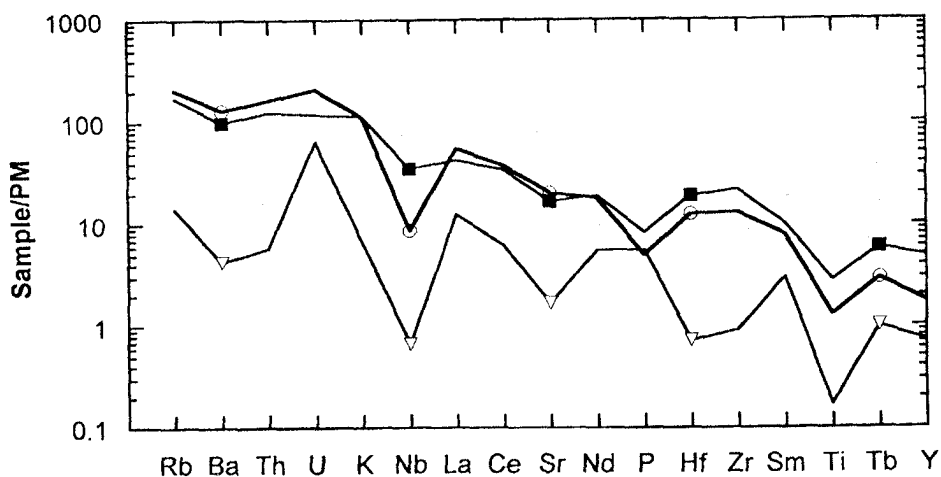

Fig. 2: Primitive Mantle (PM) normalised diagrams indicating the trace element geochemical similarity between the average Geita BIF (open triangles), average upper continental crust (solid squares) and average Geita granite (open circles). The upper crust data are from Taylor and McLennan (1981) whereas the granite data are from Maboko and Manya (unpublished data). Normalizing values are from Macdough and Sun (1995)

Figure 3 shows shale-normalised REE patterns for the BIF samples. The samples are depleted by up to an order of magnitude in the REE relative to average North American Shale (Gromet *et al.* 1984) and show nearly flat patterns which are characterised by small positive Eu anomalies and very slight negative Ce anomalies (Fig. 3). These patterns are in marked contrast to the heavy (H)REE-enriched patterns of modern sea water (Sholkovitz &

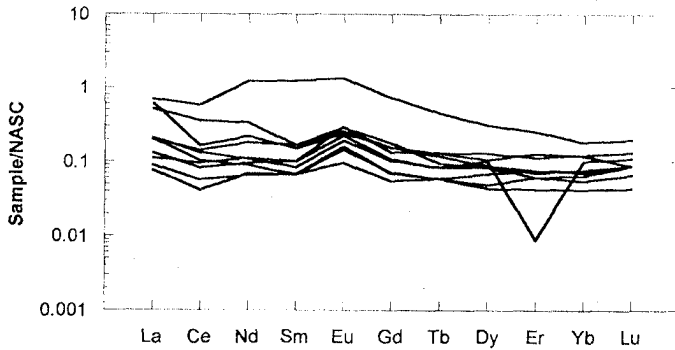Szymczak 2000) and most other Precambrian iron formations (Bau and Moller 1993).

Fig. 3: North American Shale (NASC) normalised REE patterns for the Geita BIF. The normalizing values are from Gromet *et al.* (1984)

The REE data are plotted in chondrite normalised (Normalising values after Boynton 1984) diagrams in Figure 4. All samples are characterised by light (L) REE-enriched ($(La/Yb)_N$ = 7–60: the subscript N indicates chondrite normalised values) and nearly flat to slightly depleted HREE ($(Tb/Yb)_N = 0.95$ – 2.9) patterns on which are superposed slightly positive Eu anomalies and very small negative Ce anomalies (Fig. 4). These patterns differ from the HREE-enriched trends ($(Sm/Yb)_N < 1$) which characterise most Archaean BIF (see for example Bau and Moller 1993). Apart from the positive Eu anomalies, however, the Geita BIF patterns are similar to the REE patterns of pelagic clays (Barrett 1981).
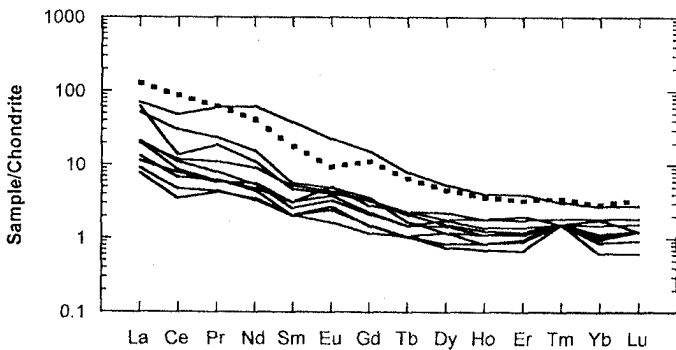

Fig. 4: Chondrite normalised REE patterns for the Geita BIF. The heavy dotted line indicates the pattern for average Geita granite and is from Maboko and Manya (unpublished data). Normalizing values are from Boynton (1984)

DISCUSSION
Origin of the BIF

Metalliferous sediments, including BIF, can form as a result of hydrothermal precipitation from seawater, diagenetic processes or physical accumulation of metal-rich detritus. Bonatti (1975) suggested that hydrothermal metal-rich deposits could be distinguished from hydrogenous deposits formed by diagenetic processes on the basis of the relative abundances of SiO_2 and Al_2O_3. On a plot of SiO_2 *versus* Al_2O_3, all the Geita BIF samples plot in the field of hydrothermal deposits suggesting that they are chemical precipitates with little or no detrital input (Fig. 5). The relative proportion of detrital, if any, to hydrothermal input in such deposits can be inferred using Fe-Ti-Mn-Al systematics (Bostrom 1973, Barret 1981, Wonder *et al.* 1988). Pure hydrothermal deposits contain very little Al and have high Fe/Ti ratios (Bostrom 1973, Marchig *et al.* 1982). Contamination of such deposits by pelagic and terrigenous deep-sea sediments enriches them in components such as Ti and Al resulting in a drastic lowering of the Fe/Ti ratio and an increase in the Al/(Al+Fe+Mn) ratio. On an Fe/Ti *versus* Al/(Al + Fe + Mn) diagram (Bostrom 1973, Barret 1981, Wonder *et al.* 1988), the Geita samples cluster on or close to the hydrothermal end of a mixing curve between hydrothermal deposits, as represented by the metal-rich sediments of the East Pacific Rise, and pelagic sediments (Fig. 6). This suggests that the major elements in the BIF are predominantly ($\geq$ ~80%) of hydrothermal origin. A predominantly hydrothermal origin is also consistent with the low Y/P_2O_5 ratios which fall in the 15 – 65 range (mean = 36 $\pm$ 10, 2 SE), similar to ratios expected in pure hydrothermal deposits but lower than ratios of >100 found in pelagic and hydrogenous deposits (Marchig *et al.* 1982). The major and trace element data, therefore, suggest that the Geita BIF, like most other Archaean and Proterozoic iron formations, were deposited from hydrothermal solutions.
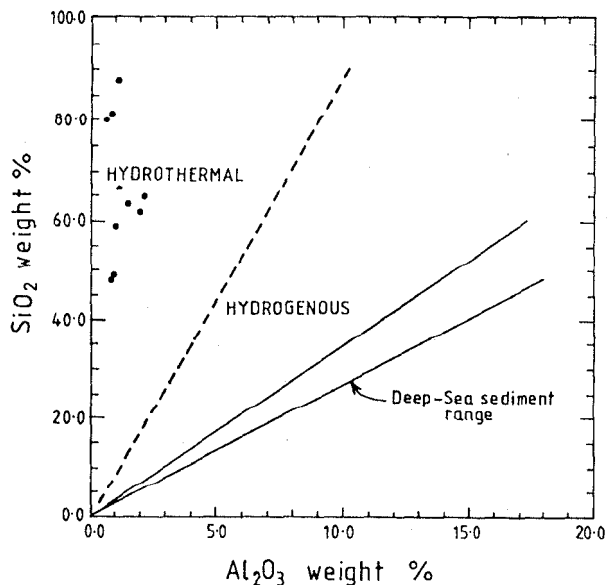
Fig. 5: SiO$_2$ *versus* Al$_2$O$_3$ discrimination diagram (after Bonatti 1975) for the Geita BIF indicating their hydrothermal affinity. Also indicated are fields for hydrogenous deposits and deep-sea sediments
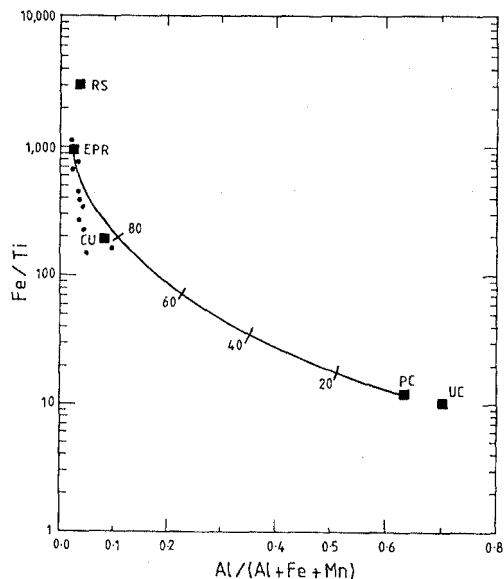

Fig. 6: Fe/Ti *versus* Al/(Al + Fe + Mn) systematics for the Geita BIF. The curve represents mixing of East Pacific Rise hydrothermal deposits (EPR) with pelagic sediments (PC) whereas the numbers indicate the approximate percentage of EPR in the mixture (adopted from Barret 1981). Also indicated are compositions for mean upper continental crust (UC, Taylor and McLennan 1981), Red Sea hydrothermal deposits (RS, Marchig *et al.* 1982) and the Cyprus umbcı (CU, Bostrom 1973)

30

Sources of the chemical components

Trace elements, and REE in particular, have been successfully used to put constraints on the relative importance of terrigenous and volcanogenic components in BIF and other Fe-rich sediments (Dymek & Klein 1988, Manikyamba & Naqvi 1995, Lottermoser & Ashley 2000). While variable, the REE patterns of BIF from different parts of the world share some important similarities. Most of them show patterns characterised by HREE enrichment $((Sm/Yb)_N < 1)$, $(La/Nd)_N > 1$ and positive Eu anomalies. These characteristics are also shared by modern deep-sea metalliferous sediments found on mid-ocean ridge flanks (Ruhlin & Owen 1986) and have been interpreted as indicating precipitation of BIF from multi-component systems consisting of variable mixtures of hydrothermal fluids containing REE leached from the basalts of the sea floor and surface marine waters, the REE signature of which resemble modern sea water (Jacobsen & Pimentel-Klose 1988, Derry & Jacobsen 1990, Bau & Moller 1993, Bau & Dulski 1996). Thus, the positive Eu anomalies are generally interpreted as reflecting the hydrothermal component whereas the HREE-enrichment reflects the influence of surface marine waters (Derry & Jacobsen 1990, Bau & Moller 1993). Similar to other Precambrian BIF, the Geita samples are characterised by slightly positive Eu anomalies $((Eu/Eu^* = 1.3 - 2.0,$ mean = 1.6$)$ and $(La/Nd)_N > 1$ $(1.1 - 5.5,$ mean = 3.0$)$ which features reflect the hydrothermal influence. In contrast to most other BIF, however, the Geita samples show strong HREE depletion $((Sm/Yb)_N = 1.9 - 6.6,$ mean = 4.1$)$. The HREE-depleted patterns of the BIF can not be explained by precipitation from a mixture of hydrothermal solutions similar to those found along modern mid-oceanic ridges or back-arc spreading centres and modern marine surface waters. Modern hydrothermal solutions are characterised by low REE abundances (pg/g levels) and patterns with large positive Eu anomalies, LREE enrichment and nearly flat to depleted HREE (Michard *et al.* 1984, Fouquet *et al.* 1993). On the other hand, modern seawater is dominated by REE from the dissolved fraction carried into the ocean by rivers. This fraction is usually characterised by HREE-enriched patterns due to fractionation processes occurring in the estuarine environment which preferentially scavenge the LREE relative to the HREE (Bau & Moller 1993, Sholkovitz & Szymczak 2000). The REE patterns of most BIF can be explained by precipitation from hydrothermal solutions that have been strongly diluted by seawater (Dymek & Klein 1988, Derry & Jacobsen 1990, Bau & Moller 1993). The seawater imparts the strong HREE enrichment (Dymek & Klein 1988) whereas the hydrothermal component is reflected in the positive Eu anomalies and the LREE enrichment. Depletion in the HREE in chemical sediments, as reflected in elevated $(Sm/Yb)_N$ ratios have been attributed to an increased contribution of particulate and colloidal components in the total REE budget (Bau & Moller 1993). The HREE-depletion in the Geita samples is similarly interpreted as indicating a detrital influence on their trace element geochemistry. A comparison of the REE patterns of samples with differing degrees of detrital contamination, as measured by different Fe/Ti ratios, suggests that an increase in the detrital component results in

higher relative abundances of the light and middle REE (Fig. 7). A detrital influence on the trace element geochemistry of the BIF is also supported by ratios of the High Field Strength Elements Zr and Hf whereby the BIF have Zr/Hf ratios (41 - 64, mean 48±5, 2 SE) which are similar to the crustal average of ~40 (Dymek & Klein 1988). A positive correlation between Al_2O_3, a known indicator of detrital contamination in chemical sediments, with some trace elements (Ti, Ga, Hf, Rb, Th and Zr) provides further evidence for a terrigenous influence on these BIF geochemistry. SiO_2 and Fe_2O_3, however, show no correlation with the trace elements possibly because the SiO_2 and Fe_2O_3 are of mixed hydrothermal and detrital parentage.
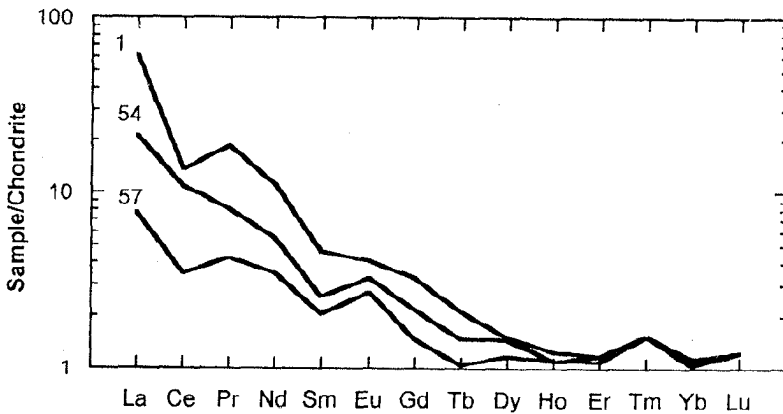

Fig. 7: Chondrite normalised REE patterns for samples with different degrees of detrital contamination as measured by different Fe/Ti ratios (187.2 for sample R1, 687.3 for sample R54 and 1024.0 for sample R57). Note the enrichment in the light and middle REE as the detrital component increases

Major rock types exposed in and around the Sukumaland Greenstone Belt that could potentially contribute detritus to the BIF depository during Neoarchaean time include metabasalts, felsic volcanics and granites. The crustal-like Zr/Hf ratios observed in the BIF, together with the lack of enrichment in Ni, Co and Sc relative to average shale preclude a significant contribution of detritus from the metabasalts (Manikyamba & Naqvi 1995). This is also consistent with the fact that the BIF have a mean $^{147}Sm/^{144}Nd$ ratio of 0.10 ± 0.01 (2 SE), indistinguishable from the ~0.11 mean value of detritus produced by the weathering of typical upper continental crustal rocks (Jacobsen & Pimentel-Klose 1988). Weathering of predominantly mafic volcanic rocks would result in significantly higher $^{147}Sm/^{144}Nd$ ratios of ~0.15 (Jacobsen & Pimentel-Klose 1988). Instead, the BIF show trace element characteristics that closely resemble those of typical Archaean granites, similar to those intruding the Nyanzian succession in the Sukumaland Greenstone Belt. This similarity, which is revealed by the parallelism of the REE and primitive mantle-normalised patterns of the BIF and granites (Figs. 2 and 4), suggests that the trace elements in the BIF were derived from detritus with

geochemical characteristics similar to that of the granites. As the granites in the Nyanzian clearly post-date BIF deposition, it is suggested that the felsic flows and pyroclastics which preceded the granitic magmatism supplied the sediments. This interpretation is supported by the presence of numerous tuffaceous horizons in the BIF (Walraven *et al.* 1994) and the fact that a trachyandesite sample interbedded with the BIF has an REE pattern that is very similar to that of both the granites and the BIF (Fig. 8). Since even samples like R57, which show minimal contamination by detrital material as revealed by their high Fe/Ti ratios (Table 1), also show HREE-depleted patterns (Fig. 7), it is proposed that some of the REE might have been derived from the hydrothermal leaching of the felsic volcanics and pyroclastics. The interbedding of the iron formations with volcanic flows provides evidence of active volcanism during the BIF deposition that could have facilitated hydrothermal leaching. Al_2O_3 is considered relatively immobile during hydrothermal leaching (Mottl & Holland 1978, Seyfried & Bischoff 1981). Thus, derivation of some of the REE by hydrothermal leaching could also explain the de-coupling of Al_2O_3 and the REE as indicated by the lack of correlation between Al_2O_3 and the total REE. The leached fraction would only contribute the REE and other trace elements to the hydrothermal solutions but not Al_2O_3.
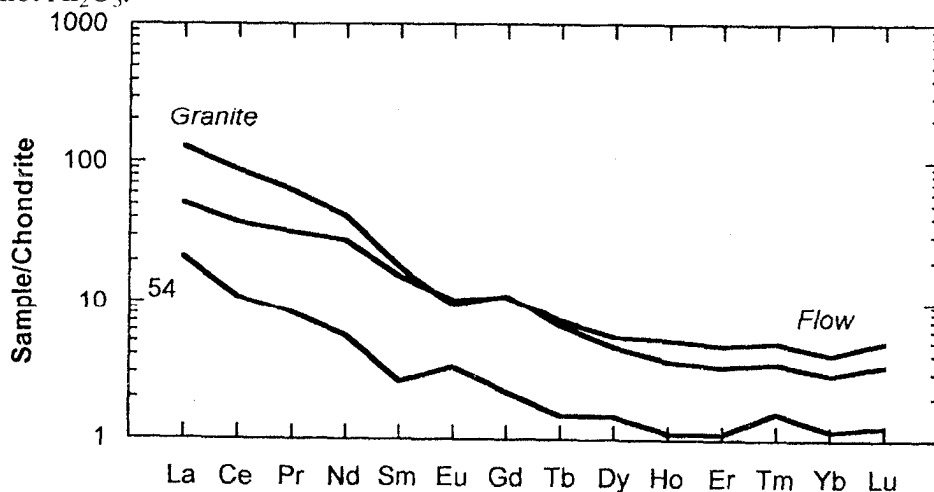

Fig. 8: Comparison of the chondrite normalised patterns for average Geita granite, least contaminated BIF (R54) and trachyandesite flow interbedded with the BIF. Even the uncontaminated BIF sample shows an REE pattern that parallels the patterns for granite and trachyandesite

CONCLUSION
The Geita BIF were precipitated from hydrothermal solutions with a maximum contamination by detrital material of ~20% by weight. The BIF are characterised by crustal-like Zr/Hf and $^{144}Sm/^{144}Nd$ ratios and REE patterns which, apart from positive Eu anomalies, are similar to those of typical

Archaean granites. This shows that, despite their lower proportions, granitic detritus probably derived from contemporaneous felsic flows and pyroclastics provided the dominant trace element geochemical characteristics of the BIF. However, even apparently detritus-free samples show the crustal geochemical signature suggesting that some of the chemical elements were derived from the hydrothermal leaching of the interbedded felsic volcanics and pyroclastics.

ACKNOWLEDGEMENT

REFERENCES

Ashley PM, Lottermoser BG and Westaway JM 1998 Iron formations and epigenetic ironstones in the Palaeoproterozoic Willyama Supergroup, Olary Domain, South Australia. *Mineralogy and Petrology* 64: 187-218

Barley ME, Pickard AL, Sylvester PJ 1997 Emplacement of a large igneous province as a possible cause of banded iron formation 2.45 Ma ago. *Nature* 385: 55-58

Barrett TJ 1981 Chemistry and mineralogy of Jurassic bedded chert overlying ophiolites in the north Appenines, Italy. *Chemical Geology* 34: 289-317

Barth H 1990 Provisional Geological Map of the Lake Victoria Gold Fields, Tanzania 1: 500000 (with explanatory notes). *Geologisches Jahrbuch* B72: 3-59

Bau M and Dulski P 1996 Distribution of ytrrium and rare earth elements in the Penge and Kuruman iron formations, Transvaal Supergroup, South Africa. *Precambrian Research* 79: 37-55

Bau M and Moller P 1993 Rare earth element systematics of the chemically precipitated iron formations and the evolution of the terrestrial atmosphere-hydrosphere-lithosphere system. *Geochimica et Cosmochimica Acta* 57: 2239-2249

Bonatti E 1975 Metallogenesis at oceanic spreading centres. *Annual Review of Earth and Planetary Sciences* 3: 401-433

Borg G 1992 New aspects on the lithostratigraphy and evolution of the Siga Hills, an Archaean granite-greenstone terrain in NW Tanzania. *Zeitschrift fur Angewandte Geologie* 38: 89-93

Borg S and Krogh T 1999 Isotopic age data of single zircons from the Archaean Sukumaland Greenstone Belt, Tanzania. *Journal of African Earth Sciences* 29: 301-312

Borg S and Shackleton RM 1997 The Tanzania and NE Zaire Cratons. In: de Wit MJ and Ashwal LD (eds). *Greenstone Belts* Clarendon Press, Oxford

Bostrom K 1973 The origin and fate of ferromanganoan active ridge sediments. *Stockholm Contributions to Geology* 27: 149-243

Boynton WV 1984 Cosmochemistry of the rare earth elements: Meteorite studies. In: Henderson P (ed) *Rare earth element geochemistry* Elsevier, Amsterdam

Derry LA and Jacobsen SB 1990 The chemical evolution of Precambrian seawater: Evidence from REEs in banded iron formations. *Geochimica et Cosmochimica Acta* 54: 2965-2977

Dymek RF and Klein C 1988 Chemistry, petrology and origin of banded iron formation lithologies from the 3800 Ma Isua supracrustal belt, West Greenland. *Precambrian Research* 39: 247-302

Fouquet Y, von Stackelberg U, Charlou JL, Erzinger J, Herzig PM, Muhe R and Wiedicke M 1993 Metallogenesis in back-arc environments: The Lau Basin example. *Economic Geology* 88: 2154-2181

Garrels RM 1987 A model for the deposition of the microbanded Precambrian iron formations. *American Journal of Science* 287: 81-106

Goodwin AM 1962 Structure, stratigraphy and origin of iron formations, Michipicoten Area, Algoma District, Ontario, Canada. *Geological Society of America Bulletin* 73: 561-586

Grantham DR, Temperley BN and McConnell RB 1945 Explanation of the geolgy of degree sheet No.17. Kahama. *Bulletin of the Geological Survey Tanganyika* (Dar es Salaam) 39 pp

Gromet LP, Dymek RF, Haskin LA and Korotev RL 1984 The "North American shale composite": its compilation, major and trace element characteristics. *Geochimica et Cosmochimica Acta* 48: 2469-2482

Halbich IW, Scheepers R, Lamprecht D, van Deventer JN and de Kock NJ 1993 The Transvaal-Griqualand West banded iron formation: geology, genesis, iron exploitation. *Journal of African Earth Sciences* 16: 63-120

Holland HD 1984 *The Chemical Evolution of the Atmosphere and Oceans.* Princeton University Press

Jacobsen SB and Pimentel-Klose MR 1988 A Nd isotopic study of the Hamersley and Michipicoten banded iron formations: the source of REE and Fe in Archaean oceans. *Earth and Planetary Science Letters* 87: 29-44

James HL 1954 Sedimentary facies of iron formation. *Economic Geology* 49: 235-291

Klemm DD 2000 The formation of Palaeoproterozoic banded iron formations and their associated Fe and Mn deposits, with reference to the Griqualand West deposits, South Africa. *Journal of African Earth Sciences* 30: 1-24

Lepp H and Goldich SS 1973 Origin of Precambrian iron formations. *Economic Geology* 59: 1025-1060

Lottermoser BG and Ashley PM 2000 Geochemistry, petrology and origin of Neoproterozoic ironstones in the eastern part of the Adelaide Geosyncline, South Australia. *Precambrian Research* 101: 49-67

Manikyamba C and Naqvi SM 1995 Geochemistry of Fe-Mn formations in the Archaean Sandur schist belt, India – mixing of clastic and chemical processes at a shallow shelf. *Precambrian Research* 72: 69-95

Marchig V, Gundlach H, Moller P and Schley F 1982 Some geochemical indicators for discrimination between diagenetic and hydrothermal metalliferous sediments. *Marine Geology* 50: 241-256

McDonough WF and Sun S-s 1995 The composition of the Earth. *Chemical Geology* 120: 223-253

Michard G, Albarede F, Michard A, Minster JF, Charlou JL and Tan N 1984 Chemistry of solutions from 13‰ N East Pacific Rise hydrothermal site. *Earth and Planetary Science Letters* 67: 297-307

Mottl MJ and Holland HD 1978 Chemical exchange during hydrothermal alteration of basalt by seawater –I: Experimental results for major and minor components of seawater. *Geochemica et Cosmochimica Acta* 42: 1103-1115

Ruhlin DE and Owen RM 1986 The rare earth element geochemistry of hydrothermal sediments from the East Pacific Rise: Examination of a seawater scavenging mechanism. *Geochemica et Cosmochimica Acta* 50: 393-400

Seyfried WE Jr. and Bischoff JL 1981 Experimental seawater-basalt interaction at 300 ‰C, 500 bars: chemical exchange, secondary mineral formation and implication for transport of heavy metals. *Geochemica et Cosmochimica Acta* 45: 135-147

Sholkovitz E and Szymczak R 2000 The estuarine chemistry of rare earth elements: comparison of the Amazon, Fly, Sepik and the Gulf of Papua systems. *Earth and Planetary Science Letters* 179: 299-309

Taylor SR and McLennan SM 1981 The composition and evolution of the continental crust: rare earth element evidence from sedimentary rocks. *Philosophical Transactions of the Royal Society of London* A301: 381-399

Walraven F, Pape J and Borg G 1994 Implications of Pb-isotopic compositions at the Geita gold deposit, Sukumaland Greenstone Belt, Tanzania. *Journal of African Earth Sciences* 18: 111-212

Wonder JD, Spry PG and Windom KE 1988 Geochemistry of manganese-rich rocks related to iron formation and sulphide deposits, Western Georgia. *Economic Geology* 83: 1070-1081